X-ray Structure and Circular Dichroism of Pure Rotamers of Bis[guanosine-5′-monophosphate(−1)](*N*,*N*,*N*′,*N*′-tetramethylcyclohexyl-1,2-diamine)platinum(II) Complexes That Have *R*,*R* and *S*,*S* Configurations at the Asymmetric Diamine

Michele Benedetti,[b] Gabriella Tamasi,[c] Renzo Cini,[c] and Giovanni Natile*[a]

Abstract: The use of a sterically hindered diamine ligand (Me_4DACH) has allowed for the first time, the isolation and characterization, both in the solid state (X-ray crystallography) and in solution (circular dichroism), of pure ΔHT rotamers of [Pt(Me_4dach)(5′-GMP)$_2$] (compounds **1** and **2** for *R*,*R* and *S*,*S* configurations of the Me_4DACH ligand, respectively). Comparison of the CD spectra obtained for each rotamer, which differ only in the chirality of the Me_4DACH ligand (*R*,*R* or *S*,*S*) or in the chirality of the HT conformation (Δ or Λ), allowed us to conclude that, in the 200–350 nm range, the contributions to the overall CD spectrum that stem from diamine chirality and diamine-induced chirality of platinum d--d transitions or from sugar chirality are negligible relative to the exciton chiral coupling that occurs for π–π* transitions of the *cis* guanines. Accurate molecular structures of **1**·10D_2O and **2**·14D_2O (conventional crystallographic agreement indexes R_1 convergent to 2.07% and 2.18%, respectively) revealed that the crystallized rotamers have a ΔHT conformation that is in agreement with all previously reported X-ray structures of [Pt(diamine)(nucleos(t)ide)$_2$] complexes. This conformation allows the 5′-phosphate to be located in proximity to the Me_4DACH ligand so that (P)O···HC(N) hydrogen-bond interactions exists in both complexes. For both structures, the canting of the guanine planes on the coordination plane is right-handed (R; canting angle (Φ) of 80.9° and 73.2°, respectively); this indicates that the canting direction is driven by the HT conformation chirality (Δ for both compounds) and not by the chirality of the carrier ligand (different for the two compounds). Density functional theory analysis of the conformational space as a function of Φ indicated a good agreement between the computed and experimental structures. The increase in energy for Φ values below 65° and 55° (for **1** and **2**, respectively) is mainly due to the short intramolecular contacts between C(8)H and the *cis* N–Me groups on the same side of the platinum coordination plane.

Keywords: antitumor agents · chiral resolution · circular dichroism · platinum · X-ray diffraction

Introduction

Rosenberg's discovery of the antitumor activity of cisplatin (*cis*-[$PtCl_2(NH_3)_2$])[1–3] represented a breakthrough in tumor chemotherapy. Cisplatin, which is highly effective in the treatment of testicular and ovarian cancers, is used in association with other antitumor drugs in the treatment of oropharingeal, bronchogenic, and cervical carcinomas, lymphoma, osteosarcoma, melanoma, bladder carcinoma, and neuroblastoma.[4]

Since the introduction of cisplatin, a large number of new platinum compounds have been prepared and tested for antitumor activity. However, only a few of them have reached clinical trials,[5] and only one, diamine(1,1-cyclobutanedicarboxylate-*O*,*O*′)platinum(II) (carboplatin), has achieved world-wide approval for routine clinical use. This new drug has a lower toxicity than cisplatin, but is unable to overcome cisplatin resistance in the same range of tumors. More recently, two other platinum compounds, namely diamine(glycolate-*O*,*O*′)platinum(II) (nedaplatin or 254-S) and (*R*,*R*)-1,2-diaminocyclohexane(oxalate-*O*,*O*′)platinum(II)

[a] Prof. G. Natile
Dipartimento Farmaco-Chimico
Università degli Studi di Bari
Via E. Orabona 4, 70125 Bari (Italy)
Fax: (+39) 080-544-2230
E-mail: natile@farmchim.uniba.it

[b] Prof. M. Benedetti
Dipartimento di Scienze e Tecnologie Biologiche ed Ambientali
Università degli Studi di Lecce
Via Monteroni, 73100 Lecce (Italy)

[c] Dr. G. Tamasi, Prof. R. Cini
Dipartimento di Scienze e Tecnologie Chimiche e dei Biosistemi
Università degli Studi di Siena
Via Aldo Moro 2, 53100 Siena (Italy)

DOI: 10.1002/chem.200305152

(oxaliplatin or L-OHP), have received approval for use in some countries, although the latter is only used for the secondary treatment of metastatic colorectal cancer.[6]

DNA is considered to be the principle target of platinum drugs. Cisplatin mainly targets DNA by binding to N7 of adjacent purines.[5–10] The resultant intrastrand adducts are thought to be the lesions that are responsible for cell death, but the mechanism of action is not entirely understood. Failure to fully understand the mechanism of antitumor activity could be responsible for the low success rate in the development of new platinum drugs able to overcome cisplatin resistance.

The *cis*-[PtA$_2$G$_2$]-type complexes (A$_2$ = two unidentate or one bidentate amine ligand, G$_2$ = two guanine derivatives that are not connected by a phosphodiester linkage) have been extensively studied as model compounds for platinum–DNA cross-links. The presence of enhanced CD signals for some *cis*-[PtA$_2$G$_2$] species was first reported in 1980,[11] and attempts were later made to interpret the results on a structural basis.[12,13] CD signals in the 200–350 nm range were thought to be the result of chiral coupling between *cis*-guanine electronic transitions. The guanine bases were assumed to be canted on the coordination plane and the Cotton-effect inversion observed was correlated with a change in the canting direction (L and R canting depends upon the handedness of two straight lines; one that connects the N7 atoms of the two coordinated guanines, and the other that passes through C8 and bisects a given guanine).

A convincing interpretation of the CD results came from recent studies of less dynamic complexes.[9,14,15] Studies with [Pt{(*S*,*R*,*R*,*S*)-Me$_2$dab}G$_2$] and [Pt{(*R*,*S*,*S*,*R*)-Me$_2$dab}G$_2$] complexes (Me$_2$DAB = *N*,*N*′-dimethyl-2,3-diaminobutane, and has four asymmetric centers at the N, C, C, and N chelate ring atoms) demonstrated a correlation between the sign of the CD signal and the chirality of the major HT form.[14,15] HT conformers have a head-to-tail orientation of the guanine bases and can have either a Δ or Λ chirality depending upon the handedness of two straight lines; one passes through the platinum center perpendicularly to the coordination plane, and the other connects the O6 atoms of the two guanines.[16,17] Furthermore, studies with the related [Pt{(*S*,*R*,*R*,*S*)-bip}G$_2$] and [Pt{(*R*,*S*,*S*,*R*)-bip}G$_2$] complexes (BIP = 2,2′-bipiperidine) indicated that a mixture of 25% ΔHT, 50% HH, and 25% ΛHT essentially had a CD spectrum that lacked any intensity. However, with time, as the HT form became dominant, the intensity of the spectrum increased. Based on the above experiments it was concluded that the sign and intensity of the CD signal reflected the conformation (Δ or Λ) and abundance of the major HT form.[18]

In the solid state, *cis*-[PtA$_2$(nucleos(t)ide)$_2$] complexes exclusively adopt the ΔHT conformation. This is not the case for guanine bases that lack the ribo(phosphate) moiety, as has been determined from the solid-state characterization of the HH rotamer and both the HT conformers (Δ and Λ).[19–21]Based on the above-mentioned observations, we argued that it should be possible to crystallize pure ΔHT rotamers of less dynamic *cis*-[PtA$_2$(nucleos(t)ide)$_2$] complexes; this would then allow the CD spectra of a single HT rotamer to be detected directly, and a more direct correlation between the CD features and the complex stereochemistry to be established.

To this end, we needed a carrier ligand for which the rotamer interconversion would be negligible, while the sample was prepared and a CD spectrum was obtained. Me$_2$DAB ligands allow a relatively fast interconversion of rotamers (although this is slow on the NMR timescale). Me$_4$DAB is a much better ligand for this purpose, but the rotamers still equilibrate after several hours. On the other hand, with Me$_4$DACH (*N*,*N*,*N*′,*N*′-tetramethyl-1,2-diaminocyclohexane), the steric hindrance from the four N–Me substituents and the ligand rigidity that arises because of the two fused rings has the effect that the puckered five-membered chelate ring of the diamine does not undergo ring inversion. The ΔHT rotamers of both [Pt{(*R*,*R*)-Me$_4$dach}(5′-GMP)$_2$] and [Pt{(*S*,*S*)-Me$_4$dach}(5′-GMP)$_2$] were isolated in the solid state and characterized by single-crystal X-ray diffraction. For the first time, the CD spectra of pure ΔHT conformers were obtained, and an accurate analysis could be made of the different factors which contribute to the overall optical activity of these types of platinum–nucleobase adducts.

Results

[Pt{(*R*,*R*)-Me$_4$dach}(5′-GMP)$_2$] (**1**) and [Pt{(*S*,*S*)-Me$_4$dach}(5′-GMP)$_2$] (**2**) were obtained by reacting the aquasulfate species [Pt(Me$_4$dach)(H$_2$O)(SO$_4$)]·H$_2$O with 5′-GMP. Each compound is present in solution as an equimolar mixture of the ΔHT and ΛHT rotamers. Spontaneous crystallization of the above compounds from water (pH ≈3 and total concentration of ≈7 mM) afforded crystals of the pure ΔHT rotamers **1** and **2**, respectively.

The ^{1}H NMR spectra of **1** and **2** are very similar and indicated that only one rotamer was present. The differences in chemical shift observed for **1** and **2** were small for both the H8 (ca. 0.07 ppm) and the N–Me protons (ca. 0.1 ppm).

UV-visible and CD spectra: The UV-visible spectra of **1** and **2** in the 185–350 nm range are practically superimposable and show two broad absorption bands: one centered at 190 nm ($\varepsilon = 5.0 \times 10^4$ M^{-1}cm^{-1}) with a shoulder at 210–220 nm, and the second centered at 259 nm ($\varepsilon = 2.6 \times 10^4$ M^{-1}cm^{-1}) with a shoulder at 285–295 nm. Furthermore, the CD spectra of **1** and **2** are also virtually identical in the 200–350 nm range (Figure 1).

After the ΔHT rotamer crystallized, each mother liquor was enriched with the ΛHT rotamer. Therefore, it was possible to obtain a good CD spectrum of the ΛHT rotamer by measuring the CD spectrum of the ΛHT-enriched solution and then subtracting the residual contribution of the ΔHT rotamer, the concentration of which was determined by ^{1}H NMR spectroscopy. The CD spectra for the ΛHT rotamers of **1** and **2** are depicted in Figures 2 and 3, respectively (bold lines). The spectra of the corresponding ΔHT rotamers are shown for comparison (dashed lines). Figures 2 and 3 also depict the average of the two spectra (dotted lines). It can be seen that, for any given Me$_4$DACH ligand chirality, the

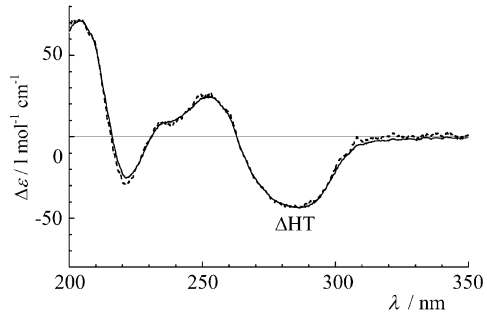

Figure 1. CD spectra of ΔHT rotamers of complexes **1** (——) and **2** (-----) in D_2O at pH = 3.

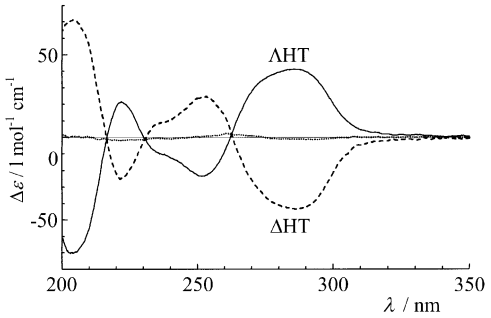

Figure 2. CD spectra of different rotamers of complex **1**: ΔHT (-----), ΛHT (——), and the average of ΔHT and ΛHT (•••••) in D_2O at pH = 3.

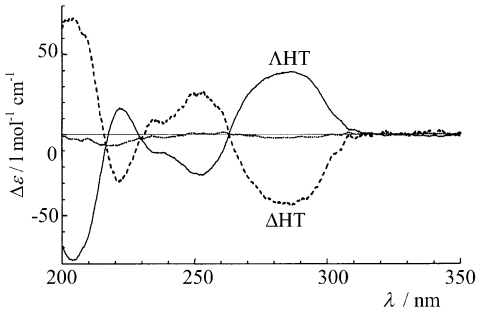

Figure 3. CD spectra of different rotamers of complex **2**: ΔHT (-----), ΛHT (——), and the average of ΔHT and ΛHT (•••••) in D_2O at pH = 3.

CD spectra of the ΛHT and ΔHT rotamers are almost perfectly symmetrical. Moreover, the CD spectra for the ΛHT conformers of **1** and **2** are also almost identical, as was observed for the ΔHT rotamers, although the diamine ligand chirality is opposite for the two compounds.

X-ray crystallography: Compounds [Pt{(*R*,*R*)-Me_4dach}(5′-GMP)$_2$] (**1**) and [Pt{(*S*,*S*)-Me_4dach}(5′-GMP)$_2$] (**2**) crystallize with 10 and 14 water molecules per platinum atom, respectively. Even though the data collections were carried out at room temperature, no appreciable efflorescence of the co-crystallized water molecules occurred, and the conventional crystallographic agreement factors were very small for both structures (Table 1).

Views of **1** and **2** are shown in Figures 4 and 5, respectively. For both structures, the metal atom sits on a crystallo-

Table 1. Selected crystal data and structure refinement parameters for ΔHT rotamers of **1**·10D_2O and **2**·14D_2O.

	1·10D_2O	**2**·14D_2O
formula	$C_{30}H_{36}D_{32}N_{12}O_{26}P_2Pt_1$	$C_{30}H_{36}D_{40}N_{12}O_{30}P_2Pt_1$
M_r	1302.2	1382.3
crystal system	monoclinic	orthorhombic
space group	*C*2 (no. 5)	$P2_122_1$ (no. 18)
a [Å]	21.254(4)	10.041(4)
b [Å]	11.535(1)	11.593(1)
c [Å]	10.550(1)	23.532(2)
α [°]	90	90
β [°]	101.31(1)	90
γ [°]	90	90
V [Å^3]	2536.3(6)	2739.3(11)
Z	4	4
ρ_{calcd} [Mg m^{-3}]	1.705	1.676
μ [mm^{-1}]	3.077	2.859
data/restraints/parameters	2607/1/321	3331/0/339
goodness-of-fit on F^2	1.065	1.147
R indices [$I > 2\sigma(I)$]	$R1 = 0.0207$, $wR2 = 0.0532$	$R1 = 0.0218$, $wR2 = 0.0572$
R indices (all data)	$R1 = 0.0207$, $wR2 = 0.0532$	$R1 = 0.0230$, $wR2 = 0.0578$

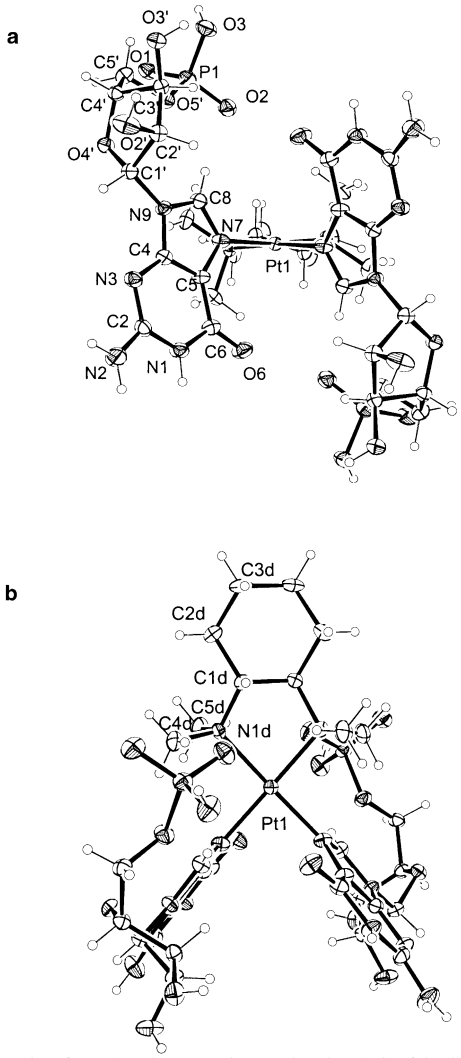

Figure 4. Ortep drawings for the complex molecule of **1** with the atom numbering scheme. Ellipsoids are drawn at 30% probability; a) the view almost parallel to the coordination plane from the G side; and b) the view almost perpendicular to the coordination plane.

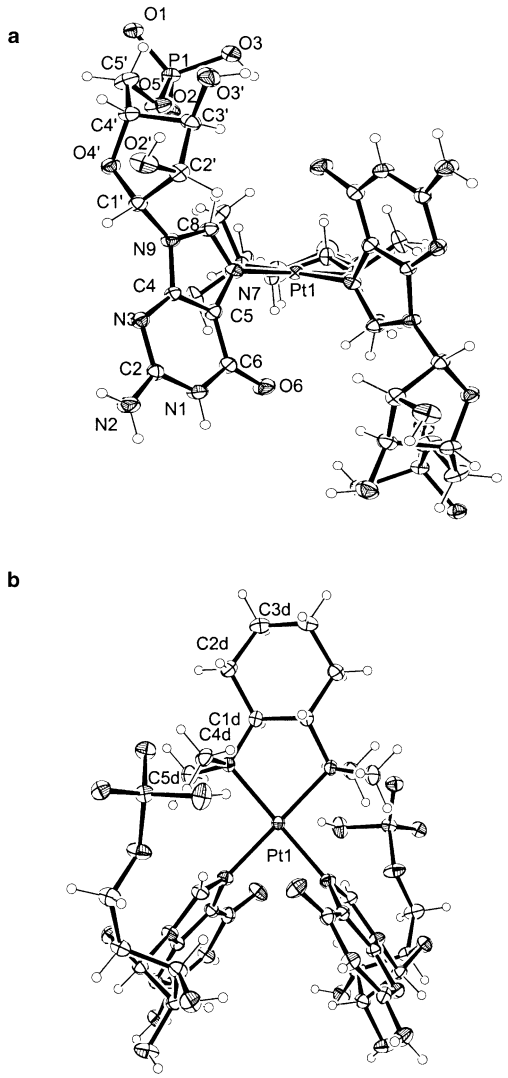

Figure 5. Ortep drawings for the complex molecule of **2** with the atom numbering scheme. Ellipsoids are drawn at 30% probability: a) the view almost parallel to the coordination plane from the G side; and b) the view almost perpendicular to the coordination plane.

graphic twofold axis. Bond lengths and angles are listed in Tables 2 and 3, respectively, while selected torsion angles, pseudo-rotation phase angles, and maximum torsion angles are reported in Table 4.

The coordination sphere: The coordination sphere is square-planar for both **1** and **2**. The metal center is linked to the two nitrogen atoms of the Me_4DACH ligand [N(A)] and to the N7 atoms of the two 5′-GMP ligands [N(G)]. The Pt–N(A) bond lengths are slightly longer (2.049(8) and 2.057(4) Å for **1** and **2**, respectively) than the Pt–N(G) bond lengths (2.028(9) and 2.040(3) Å for **1** and **2**, respectively). These values compare well with the corresponding bond lengths found for $[Pt^{II}(dap)(Me\text{-}5'\text{-}GMP)_2]$ (**3**) (DAP = 1,3-diaminopropane, Me-5′-GMP = 5′-guanosine monophosphate methyl ester, Pt–N(A) = 1.993 Å and Pt–N(G) = 2.021 Å)[22] and $[Pt^{II}(dae)(5'\text{-}GMP)_2]$ (**4**) (DAE = 1,2-diaminoethane, Pt–N(A) = 2.037 Å and Pt–N(G) = 2.046 Å).[23] The N(G)-Pt-N(G) bond angles are 86.9(5)° and 86.1(2)°

Table 2. Selected bond lengths [Å] for ΔHT rotamers of **1**·10 D_2O and **2**·14 D_2O.

	1·10 D_2O	**2**·14 D_2O		**1**·10 D_2O	**2**·14 D_2O
Pt1–N7	2.028(9)	2.040(3)	N3–C4	1.341(7)	1.343(6)
Pt1–N1d	2.049(9)	2.057(4)	N7–C8	1.313(10)	1.314(8)
P1–O1	1.494(7)	1.511(3)	N7–C5	1.395(9)	1.389(7)
P1–O2	1.486(5)	1.493(3)	N9–C8	1.357(7)	1.357(6)
P1–O3	1.598(5)	1.576(4)	N9–C4	1.378(6)	1.393(6)
P1–O5′	1.609(4)	1.596(3)	N9–C1′	1.465(6)	1.463(6)
O6–C6	1.228(7)	1.234(6)	N1d–C5d	1.493(10)	1.481(7)
O2′–C2′	1.408(10)	1.419(6)	N1d–C1d	1.493(10)	1.510(6)
O3′–C3′	1.399(7)	1.404(6)	N1d–C4d	1.508(9)	1.483(8)
O4′–C1′	1.420(6)	1.412(5)	C4–C5	1.377(8)	1.374(7)
O4′–C4′	1.443(6)	1.449(5)	C5–C6	1.424(7)	1.423(6)
O5′–C5′	1.415(9)	1.439(6)	C1′–C2′	1.525(7)	1.537(7)
N1–C2	1.354(8)	1.357(6)	C2′–C3′	1.529(7)	1.529(7)
N1–C6	1.394(8)	1.395(6)	C3′–C4′	1.521(8)	1.538(7)
N2–C2	1.340(8)	1.326(7)	C4′–C5′	1.521(9)	1.502(6)
N3–C2	1.328(7)	1.343(6)			

Table 3. Selected bond angles [°] for ΔHT rotamers of **1**·10 D_2O and **2**·14 D_2O.[a]

	1·10 D_2O	**2**·14 D_2O		**1**·10 D_2O	**2**·14 D_2O
N7#2-Pt1-N7	86.9(5)	86.1(2)	N2-C2-N1	117.6(5)	117.7(4)
N7#2-Pt1-N1d	173.5(4)	179.6(2)	N3-C4-C5	129.4(5)	130.2(4)
N7-Pt1-N1d	94.6(2)	94.3(1)	N3-C4-N9	124.2(5)	123.5(4)
N1d-Pt1-N1d#2	84.6(5)	85.3(2)	C5-C4-N9	106.4(5)	106.3(4)
O2-P1-O1	116.2(3)	118.8(2)	C4-C5-N7	108.4(5)	108.6(4)
O2-P1-O3	111.3(3)	110.0(2)	C4-C5-C6	118.8(5)	118.5(4)
O1-P1-O3	108.4(3)	105.4(2)	N7-C5-C6	132.8(6)	132.7(5)
O2-P1-O5′	107.9(2)	106.4(2)	O6-C6-N1	121.1(5)	120.6(4)
O1-P1-O5′	109.8(3)	109.8(2)	O6-C6-C5	128.6(6)	128.7(5)
O3-P1-O5′	102.4(4)	105.7(2)	N1-C6-C5	110.3(5)	110.5(4)
C1′-O4′-C4′	110.5(4)	109.8(4)	N7-C8-N9	111.5(6)	111.5(4)
C5′-O5′-P1	116.1(4)	119.1(3)	O4′-C1′-N9	108.1(4)	108.9(4)
C2-N1-C6	126.2(5)	126.4(4)	O4′-C1′-C2′	107.8(4)	107.0(4)
C2-N3-C4	111.2(5)	110.6(4)	N9-C1′-C2′	113.9(4)	112.3(4)
C8-N7-C5	106.4(7)	106.8(4)	O2′-C2′-C1′	106.7(4)	105.1(4)
C8-N7-Pt1	123.8(6)	125.8(4)	O2′-C2′-C3′	111.8(4)	112.3(4)
C5-N7-Pt1	129.6(6)	127.1(5)	C1′-C2′-C3′	104.4(4)	102.0(4)
C8-N9-C4	107.2(4)	106.8(4)	O3′-C3′-C4′	109.3(4)	110.9(4)
C8-N9-C1′	128.1(4)	128.9(4)	O3′-C3′-C2′	114.7(5)	114.4(4)
C4-N9-C1′	124.6(4)	123.5(4)	C4′-C3′-C2′	103.5(4)	100.4(4)
C5D-N1d-Pt1	106.3(5)	110.9(3)	O4′-C4′-C3′	106.8(4)	109.7(4)
C1D-N1d-Pt1	109.2(5)	109.0(3)	O4′-C4′-C5′	108.0(5)	117.4(4)
C4D-N1d-Pt1	114.1(5)	107.4(3)	C3′-C4′-C5′	115.6(5)	103.7(3)
N3-C2-N2	118.3(5)	118.6(5)	O5′-C5′-C4′	108.2(5)	109.2(4)
N3-C2-N1	124.1(5)	123.6(5)			

[a] #2: −x, y, −z for **1** and **2**. Translations along *x*, *y*, *z* are not taken into account.

Table 4. Selected torsion angles [°], pseudo-rotation phase angles {*P*, $\tan P = [(\nu_4 + \nu_1) - (\nu_3 + \nu_0)]/2\nu_2(\sin 36° + \sin 72°)$}, and maximum torsion angle (ν_{max}, $\nu_2/\cos P$) for ΔHT rotamers of **1**·10 D_2O and **2**·14 D_2O.

		1·10 D_2O	**2**·14 D_2O
χ	C4-N9-C1-O4′	−129.5	−140.5
ν_0	C4′-O4′-C1′-C2′	1.0(5)	−1.3(5)
ν_1	O4′-C1′-C2′-C3′	−16.9(5)	−23.9(5)
ν_2	C1′-C2′-C3′-C4′	25.3(5)	37.8(4)
ν_3	C2′-C3′-C4′-O4′	−25.4(5)	−39.4(4)
ν_4	C3′-C4′-O4′-C1′	15.7(5)	25.9(5)
P		16.6	20.2
ν_{max}		26.4	40.3
α	O3-P1-O5′-C5′	63.8(5)	95.4(4)
β	P1-O5′-C5′-C4′	−165.3(4)	−168.3(3)
γ	O5′-C5′-C4′-C3′	57.9(7)	64.8(5)

for **1** and **2**, respectively. These values are significantly smaller than those found for **3** (90.1°)[22] and **4** (89.1°).[23] The metal center lies in the plane of the four donors, but there is a tetrahedral distortion, which is greater for **1** than for **2** (the two amine nitrogen atoms are displaced by ± 0.115(2) Å for **1** and ±0.004(2) Å for **2** from the coordination plane). As expected, the conformation of the five-membered chelate ring is λ for **1** and δ for **2** (δ and λ correspond to the right and left-handedness of two straight lines; one connects the two nitrogen atoms, and the other connects the two carbon atoms of the chelate ring). The pucker of the five-membered ring is a pure twist (T, C_2 symmetry) for both compounds. However, the ring in compound **2** is slightly more puckered than that in **1** (q_2: 0.407(7) and 0.442(5) Å for **1** and **2**, respectively).[24]

The GMP ligands: Both complexes have a ΔHT conformation for the guanine systems. The guanines are canted on the coordination plane and the dihedral angles (Φ) between the purine plane (only the endocyclic atoms have been considered) and that of coordination (plane of the four donors) are 80.9(4)° for **1** and 73.2(2)° for **2** (note that the given Φ angles are close to the torsion angles C8-N7-Pt-*cis*-N(A), which are 86.6(3)° and 79.1(2)° for **1** and **2**, respectively). The metal center is displaced from the guanine planes by 0.0755(1) and 0.1198(1) Å for **1** and **2**, respectively. The exocyclic N2 and O6 atoms are displaced from the mean guanine planes by 0.056(6) and 0.062(5) Å for **1** and 0.084(5) and 0.054(4) Å for **2**.

Bond lengths and angles for the guanine systems are in agreement with values previously reported.[22,23] The C2-N1-C6 bond angle is 126.2(5)° and 126.4(4)° for **1** and **2**, respectively, and is consistent with N1 being protonated. The conformation around the glycosidic bond N9–C1′ is −anti-clinal (torsion angle (χ) for C4-N9-C1′-O4′ is −129.5° and −140.5° for **1** and **2**, respectively).[25,26] The conformation of the ribose ring can be described as almost pure C3′-*endo* (^{3}E, envelope-C3′) when the plane defined by C1′, C4′, and O4′ is considered. The displacement of C3′ from this plane in the direction of C5′ is −0.393(5) and −0.654(5) Å for **1** and **2**, respectively. The C2′ atom in **1** has a small amount of *exo* character (deviation of 0.025(5) Å), while in **2** it has *endo* character (deviation of −0.032(5) Å). This analysis is confirmed by the pseudo-rotation phase angle P, which is calculated from the endocyclic sugar torsion angles.[25,26] The value of P is 16.6° for **1** and 20.0° for **2** (18° for pure C3′-*endo*). The fact that **2** is puckered to a larger extent than **1** is evidenced by the ν_{max} values (26.4° for **1** and 40.3° for **2**).[25,26] Bond lengths and angles for the ribose systems are normal for both compounds.

The terminal P–O bond lengths (O1, O2, and O3) are 1.494(7), 1.486(5), and 1.598(5) Å, respectively for **1**, and 1.511(3), 1.493(3), and 1.576(4) Å, respectively for **2**. The longer P–O3 bond length indicates that only this oxygen atom is protonated. The bond angles around the phosphorus atom fall in the range 102.4(4)–116.2(3)° for **1** and 105.4(2)–118.8(2)° for **2**. The torsion angle α (O3-P1-O5′-C5′) has a +gauche, +syn-clinal, and +sc conformation for **1** (63.8(5)°), but an +anti-clinal and +ac conformation for **2** (95.4(4)°). The torsion angle β for both compounds (P1-O5′-C5′-C4′) has an −anti-periplanar conformation (−165.3(4) and −168.3(4)° for **1** and **2**, respectively), whereas the torsion angle γ (O5′-C5′-C4′-C3′) has a +gauche, +syn-clinal, and +sc conformation (57.9(7)° and 64.8(5)° for **1** and **2**, respectively).

The Me_4DACH ligand: The conformation of the Me_4DACH ligand is an almost pure chair for **1** (θ = 5.2(7)°),[24] and has a pucker amplitude of Q_T = 0.617(9) Å (0.630 Å for pure cyclohexane). The conformation of **2** is mainly that of a chair, but it does also have a half-chair component (θ = 160.4(9)°, ϕ = −105(2)°).[24] Bond lengths and angles are normal.

Intramolecular interactions (O···H–C): Relatively short intramolecular distances occur for the following atoms: the guanine oxygen O6 and the C8–H of the *cis* guanine (O6···C8 distance is 3.291 Å and the O6···H–C8 angle is 115° for **1**, while for **2** these values are 3.096 Å and 112°, respectively); the sugar oxygen O5′ and the C8–H of the same nucleotide (O5′···C8 distance is 3.258 Å and the O5′···H–C8 angle is 143° for **1**, while for **2** these values are 3.623 Å and 140°, respectively); and the phosphate oxygen O2 and the *cis*-N–Me (O2···C4d distance is 3.479 Å and the O2···H–C4d angle is 173° for **1**, while for **2** these values are 3.148 Å and 96°, respectively).

Intermolecular interactions (N,O–H···O): The O6 atom has a strong intermolecular contact distance to a co-crystallized water molecule: O6···O2W (x−0.5, y−0.5, z) = 2.844(7) Å for **1**; and O6···O5W (x, y, z) = 2.772(6) Å for **2**. The N1 atom has a strong intermolecular hydrogen bond to a phosphate oxygen atom of a neighboring molecule (N1···O1 (x−0.5, y+0.5, z) = 2.663(8) Å and N–H···O = 161.0(4)° for **1**, N1···O1 (−x+1.5, −y, z+0.5) = 2.797(5) Å and N–H···O = 157.1(3)° for **2**). The N2 amine group is involved in a variety of intermolecular hydrogen bonds with neighboring oxygen atoms. In particular, the phosphate O1 (x−0.5, y+0.5, z), the water O1W (−x+1, y, −z+1) and O4W (−x+1, y, −z+1), and the ribose O2′ (−x+1, y, −z+1) oxygen atoms are involved for **1** (shortest contact, N2···O1W = 3.149(8) Å and N–H···O = 129.9(5)°). For compound **2**, the phosphate O3 (−x+1.5, −y, z+0.5) and O1 (−x+1.5, −y, z+0.5), and the water O1W (x+0.5, −y, −z+0.5) and O6W (−x+1, y−1, −z) oxygen atoms are involved (shortest contact, N2···O3 = 2.980(6) Å and N–H···O = 146.7(4)°). The ribose O2′ atom has strong hydrogen bonds with two water molecules, namely O2W (x, y, z) (O···O = 2.842(8) Å) and O4W (x, y, z) (O···O = 2.807(9) Å) for **1**, and O4W (x, y−1, z) (O···O = 2.703(6) Å) and O1W (−x+1.5, −y, z−0.5) (O···O = 2.835(6) Å) for **2**. The ribose O3′ atom has hydrogen bond interactions with O1W (x, y, z) (O···O = 2.90(1) Å) and O2 (−x+1.5, y+0.5, −z+2) (O···O = 2.680(5) Å) for **1**, and O1 (x−0.5, −y, −z−0.5) (O···O = 2.849(6) Å) for **2**. Oxygen O4′ has a short contact with O3W (−x+1.5, y−0.5, −z+1) (O···O = 2.854(6) Å) in **1** and with O3W (−x+1, y, −z) (O···O = 2.963(6) Å) in **2**. The selected hydrogen bonds for both compounds in which the phosphate oxygen atoms are involved is shown in Figure 6. It should be noted that the

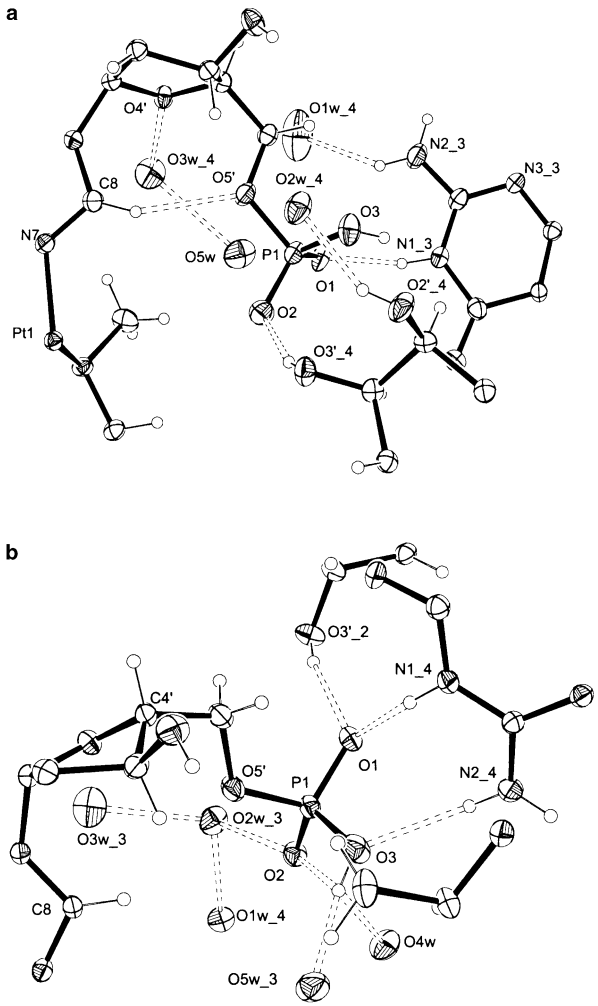

Figure 6. A depiction of all the atoms located within 6 Å of the P1 atom for **1** (a) and **2** (b). For clarity, only selected atoms are labeled. The symmetry operations are as follows (translation along *x*, *y*, *z* are not taken into account): for **1** #3, *x*+0.5, *y*+0.5, *z*; #4, −*x*+0.5, *y*+0.5, −*z*; for **2** #2, *x*+0.5, −*y*, − *z*+0.5; #3, −*x*, *y*, −*z*; #4, −*x*+0.5, −*y*, *z*+0.5.

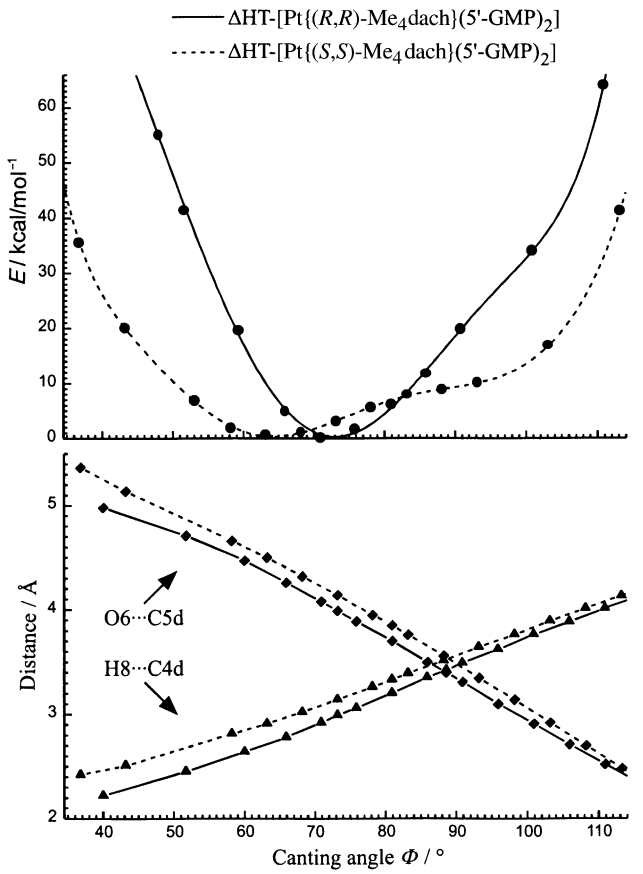

Figure 7. Computed total electronic energy as a function of the canting angle Φ. The single-point calculations were carried out through the DFT–Becke3LYP methods using the Lanl2dz basis set for all the atoms. Selected intramolecular contact distances as a function of Φ, for both **1** and **2**, are also represented.

distances between hydrogen-bonded N,O(H)···O atoms are about 2.85 Å, while those between C(H)···O atoms were about 3.30 Å.

Density functional theory (DFT) analysis: To evaluate the relative stability of molecules **1** and **2** as a function of the canting angle (Φ), preliminary single-point computations were performed by DFT methods (ab initio RHF level calculations were also carried out for comparative purposes). The total electronic energy of **1** and **2** versus Φ are shown in Figure 7.

The computed minimum energy for **1** is at $\Phi = 70.9°$, and is not far from the value found in the solid state (80.9°). The difference between the total electronic energy for the two angles is small (5.949 kcal mol^{-1}) and suggests that intermolecular hydrogen bonds (for instance, with water molecules) may be responsible for small changes ($\pm 10°$) in canting angles. The computed minimum of energy for **2** is at $\Phi = 63.2°$, and is 2.485 kcal mol^{-1} lower than the electronic energy computed for the Φ value found in the solid-state structure (73.2°). The electronic energy profile as a function of Φ has a narrower shape for **1** than for **2**, and the energy increases considerably (some 10 kcal mol^{-1} above the minimum) for Φ values outside the range 65–85° for **1** and 55–95° for **2**. The increase in energy for Φ values below 65° and 55°, for **1** and **2**, respectively, is mainly due to the short intramolecular distances between C8–H and the *cis*-N–Me groups on the same side of the platinum coordination plane, while the increase in energy for Φ values above 85° and 95° is due to the short intramolecular distances between O6 and the *cis*-N–Me groups on the same side of the platinum coordination plane.

Discussion

ΔHT compound conformation: The results obtained for the two compounds investigated confirm the general observation that the ΔHT form dominates for G nucleos(t)ides in the solid state.[16,22,23,27,28] However, two ΔHT subforms, which differ only in the canting direction (either right-handed (R) or left-handed (L) Figure 8) are possible. For a right-hand canted ΔHT rotamer (b in Figure 8), the six-membered ring of each guanine leans towards the *cis*-guanine. We call this the "six-in" conformation. For a left-hand

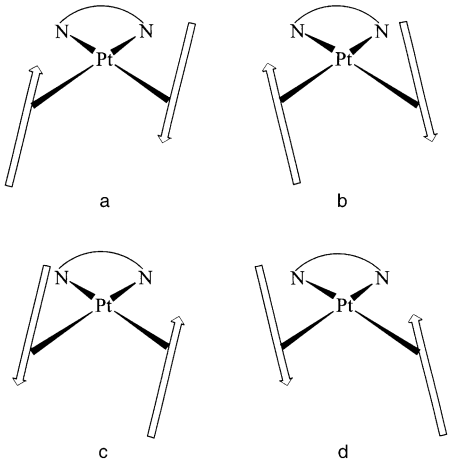

Figure 8. The ΔHT and ΛHT conformations, and their L and R subforms for *cis*-[PtA_2G_2] complexes. The arrows represent an N7-bound G in which the arrow head points toward the H8 atom: a) L-ΔHT; b) R-ΔHT; c) L-ΛHT; and d) R-ΛHT.

canted ΔHT rotamer (a in Figure 8), the six-membered ring of each guanine leans towards the *cis*-amine. We call this the "six-out" conformation. It should be noted that for *cis*-G dinucleos(t)ide adducts of platinum, all the ΔHT type solid-state structures have a right-handed canting that leads to a "six-in" conformation.

Previous studies on C_2-symmetrical diamine ligands that have an alkyl substituent as well as one proton on each nitrogen atom, such as Me_2DAB and bip,[29,30] demonstrated that two factors contributed to the stability of the HT rotamers: the dipole–dipole interaction between the guanine bases which favors the "six-in" conformation, and the steric interactions between each purine and *cis*-amine. Therefore, greater stability was observed for HT rotamers in which the H8 of each purine and the *cis*-*N*-alkyl substituent are on opposite sides of the coordination plane. In these instances, the degree of canting was greater and the dipole–dipole interaction was more favorable. Highly canted "six-in" conformations are generally preferred for [$Pt(Me_2dab)G_2$] and [$Pt(bip)G_2$] complexes in water, and are easily assigned from the chemical shift of the H8 protons, because in the most abundant HT rotamer they appear at a lower field than in the less abundant HT rotamer. The more the "six-in" conformer is canted, the less shielded is the H8 of a given guanine from the magnetic field of the *cis*-purine.

Based on the above considerations, it is not surprising that the "six-in" conformation is also preferred in the solid state of all the *cis*-nucleos(t)ide adducts of platinum so far investigated.

A "six-in" conformation is also possible for an L-canted ΛHT rotamer (c in Figure 8). Therefore, the R-canted ΔHT rotamers characterized for *cis*-G dinucleos(t)ide adducts of platinum in the solid state must be a consequence of the ribose substituent. A ΔHT orientation of the G's combined with a preferential *anti* conformation of the nucleos(t)ides directs the 5′-terminus of the ribose towards the *cis*-amine. This conformation then appears to be stabilized by intramolecular interactions, as observed in the crystal structures of **1**–**4**.[31]

In the presence of non-ribose N9-substituents at guanine, both the Δ and ΛHT rotamers have been observed in the solid state. Moreover, the "six-in" conformation is no longer exclusive; the "six-out" conformation is regularly seen,[19] and occasionally, the HH conformer has also been observed.[20,21] Therefore, it appears that a different crystal-packing basis can favor the crystallization of different *cis*-[PtA_2G_2] rotamers, in particular, when the N9-substituted guanine bases have less stringent sterochemical requirements.

Canting angle: The degree of canting increases as the dihedral angle between the guanine planes and that of coordination (Φ) decreases. In the related complexes **3** and **4**, the dihedral angles between the guanines and the coordination planes are 53° and 48°, respectively. The Φ values for **1** and **2** are 80.9° and 73.2°, respectively. The larger Φ values found for the Me_4DACH compounds are a direct consequence of the steric hindrance exerted by the methyl substituents on the diamine nitrogen atoms. The overall crystallographic data clearly indicate that the steric repulsion between each guanine and *cis*-amine group is greater than that between the two *cis*-guanines. For instance, the N(A)-Pt-N(G) angles (94.6° for **1** and 94.3° for **2**) are much larger than the N(G)-Pt-N(G) angles (86.9° for **1** and 86.1° for **2**). The latter are comparable to those of the chelate diamine N(A)-Pt-N(A) (84.6° for **1** and 85.3° for **2**).

The present study allowed us to determine the specific interaction that is responsible for the smaller canting observed in compounds **1** and **2** relative to **3** and **4**, which occurs between the guanine base and the *cis*-amine ligand. As a result of the "six-in" conformation, the O6 atom of each guanine leans towards the *cis*-guanine. Therefore, our attention can be directed solely upon the interaction that occurs between each guanine H8 proton and the *cis*-amine. The non-bonding distances between the guanine H8 proton and the *cis*-N–Me carbon C4d atom are 3.138 and 3.200 Å for **1** and **2**, respectively. In both cases, the H8···C4d distances are close to the sum of the van der Waals radii (1.20 and 2.16 Å for H and Me, respectively).[32] Therefore, the steric interactions between H8 and the *cis*-N–Me are responsible for the Φ angle being much greater in compounds **1** and **2** than in **3** and **4**, in which there are no methyl substituents on the *cis*-amine nitrogen atoms.

The smaller canting that is observed for **1** relative to **2** also deserves a brief discussion. The two N–Me groups on each nitrogen atom are non-equivalent. One is more axial and the other is more equatorial in character. The axial/equatorial character can be quantified by the N(A)-Pt-N(A)-C(Me) torsion angles. For the "quasi axial" methyl groups, the torsion angles are 108.0° for **1** and −108.9° for **2**, while for the "quasi equatorial" methyl groups they are −134.1° for **1** and 132.4° for **2**. In **1**, the H8 atoms are found beside the "quasi equatorial" N–Me groups. Similarly, in **2** the H8 atoms are located beside the "quasi axial" N–Me groups. In compound **1**, the canting is sufficiently small enough that the H8···*cis*-N–Me distance corresponds to the sum of the van der Waals radii. Therefore, the smaller canting observed in compound **1** relative to **2** is probably a

result of the different orientation of the N–Me group with respect to H8, which is "quasi equatorial" in **1** and "quasi axial" in **2**.

DFT analysis: The stability of complexes **1** and **2** as a function of the canting angle (Φ) was also evaluated through theoretical calculations. It is interesting to note that for a given degree of canting the O6···C5d and H8···C4d distances are shorter in compound **1** (H8 and the "quasi equatorial" N–Me, O6 and the "quasi axial" N–Me) than in compound **2** (H8 and the "quasi axial" N–Me, O6 and the "quasi equatorial" N–Me). As a result, the energy profile as a function of the canting angle has a narrower shape in **1** than in **2**. Low-energy values are observed for $65° < \Phi < 85°$ in **1**, and for $55° < \Phi < 95°$ in **2**. The increase in energy for Φ close to the lower limit is mainly due to the short intramolecular distances between C8–H and C4d–H_3, while the increase in energy for Φ close to the upper limit is due to steric interactions between O6 and C5d–H_3. The lowest energy computed conformations had Φ values that were about 10° lower than those found in the crystal structures. It is possible that intermolecular interactions are responsible for the observed differences. However, it is also possible that interactions between C8–H and *cis*-N–Me are underestimated in the theoretical calculations. It should be noted that H8···C4d distances observed in the crystal structures of **1** and **2** are slightly shorter than the estimated values for the sum of the van der Waals radii.

CD spectroscopy: As previously described, the presence of enhanced CD signals for some *cis*-[PtA_2G_2] complexes was first reported in 1980,[11] and attempts were later made to interpret these results on a structural basis.[12,13] Studies on the less dynamic [Pt(CCC)G_2] complexes (CCC = chirality-controlling chelates) allowed the concentration of different rotamers in solution to be determined, and as a result, the CD spectra of individual rotamers could be simplified by correlating changes in the rotamer populations (as a function of reaction time or pH) with the corresponding changes in CD signals.[33] HT rotamers were found to have far stronger CD signals than HH rotamers. Moreover, ΔHT and ΛHT rotamers had opposite Cotton effects. However, a full interpretation of the CD spectra of platinum nucleotide adducts is complicated by the possibility that contributions may arise from several sources: the carrier ligand, the metal, the ribose, or the nucleic bases. The present investigation has allowed us to separately evaluate the different contributions.

As shown in Figure 1, the CD spectra of the ΔHT rotamers of the [Pt{(*R*,*R*)-Me_4dach}(5′-GMP)$_2$] and [Pt{(*S*,*S*)-Me_4dach}(5′-GMP)$_2$] complexes are almost perfectly superimposable in the 200–350 nm range, despite the fact that they have opposite diamine chirality. Therefore, the contribution to the overall CD spectrum that stems from diamine chirality and diamine-induced chirality of platinum d–d electronic transitions is negligible. This is not surprising, since the typical electronic transitions for the diamine moiety fall in the far UV region. Moreover, the Cotton intensities observed by Saito and co-workers around 258 and 284 nm for the d–d transitions in complexes such as [Pt{(*R*,*R*)-dach}$(NH_3)_2$] and [Pt{(*S*,*S*)-dach}$(NH_3)_2$] are negligible in comparison to the overall Cotton effects observed in compounds **1** and **2**.[34]

Furthermore, the ribose contributions to the overall Cotton effect are also negligible, as can be seen from a comparison of the CD spectra of species that are enantiomeric at every chiral carbon apart from those in the sugar moiety (e.g., compare the spectra of ΔHT **1** and ΛHT **2**, or the spectra of ΛHT **1** and ΔHT **2**). These pairs of CD spectra are once again, within experimental error, perfectly symmetrical. As for aliphatic diamines, the ribose electronic transitions have σ–σ* character and typically fall in the far UV spectral region.

Exciton chiral coupling between π→π* transitions of *cis*-guanines: Since it has been demonstrated that diamine and ribose chirality, as well as diamine-induced chirality of the platinum d–d electronic transitions do not significantly contribute to the CD spectra of HT rotamers in the near UV-visible region, the observed Cotton effects in the 200–350 nm range must stem from intramolecular exciton chiral coupling between electron transition moments of the *cis*-guanines.[33,35] Qualitative application of the exciton-coupling theory in the interpretation of the CD spectra of *cis*-[PtA_2G_2] complexes predicts that in going from ΔHT to ΛHT the Cotton effects will be inverted. This occurs because the chirality of the coupled π→π* electronic transitions of the two purines inverts when the disposition of the nucleic bases is changed from ΔHT to the symmetrical ΛHT conformation. Moreover, if we increase the canting of the ΔHT and ΛHT rotamers, the Cotton effects will generally decrease. In fact, the Cotton effects are non-existent when the two guanines become coplanar with the coordination plane. These simple considerations are able to explain the two major differences observed in the CD spectra of compounds **1** and **2**, which contain tertiary amine ligands, and those of analogous [Pt(Me_2dab)G_2] and [Pt(bip)G_2] complexes, which contain secondary amine ligands. Firstly, for [Pt(CCC)G_2] complexes, the CD spectra for a pair of ΔHT and ΛHT rotamers are not perfectly symmetrical, as is the case for [Pt(Me_4dach)G_2] species. Secondly, the CD spectra of [Pt(CCC)G_2] species are generally weaker.

In complexes that contain CCC ligands, the nucleobase canting is rather different for the ΔHT and ΛHT rotamers (there is a large dispersion of the H8 resonances). In the most abundant HT rotamer, the nucleobase canting in a "six-in" conformation is large because there is no steric hindrance between the guanine H8 and the *cis*-amine N–H on the same side of the platinum coordination plane. On the other hand, in the less abundant HT rotamer, the nucleobase canting in a "six-in" conformation is limited by steric interactions between guanine H8 and the *cis*-N–Me group. In contrast, the nucleobase canting for both HT rotamers of **1** and **2**, in which the guanine H8 hydrogen atoms are on the same side as the *cis*-amine N–Me groups, is comparable (and rather small). In light of this, the CD spectra of ΔHT and ΛHT rotamers are expected to be very symmetrical for compounds **1** and **2** (equally canted ΔHT and ΛHT rotamers), but rather unsymmetrical for compounds that contain

CCC ligands (different degree of canting within each pair of ΔHT and ΛHT rotamers).

The fact that CD signals are generally stronger for compounds **1** and **2** than for compounds that contain CCC ligands can also be explained on the basis of structural considerations. We have already pointed out that the degree of canting in **1** and **2** is much smaller than in **3** and **4**, because in the former pair of compounds steric repulsion exists between each guanine H8 and the N–Me of the *cis*-amine, and this repulsion increases as the degree of canting increases. This steric repulsion is absent in **3** and **4**, as well as in the major HT rotamer of [Pt(CCC)G_2] complexes (all contain the guanine H8 on the same side of the platinum coordination plane as the N–H of the *cis*-amine). Therefore, the degree of canting is expected to be greater in the major rotamer of CCC complexes than in compounds **1** and **2**, and as a consequence, the former complexes are expected to have weaker CD spectra.

Conclusion

Compounds **1** and **2** are unique, because the pure ΔHT rotamers that crystallize are very stable in solution, and their CD spectra can be detected before any equilibration of rotamers takes place. In all other studies, both HT rotamers were at equilibrium in solution, and in order to observe a CD spectrum, the two HT rotamers had to be present in different concentrations. This could be attained either by using chiral carrier ligands, which favor one HT rotamer over the other, or by introducing guanine substituents at N9; this gives rise to different interligand interactions for the two HT rotamers.

X-ray investigations have demonstrated that in Me_4DACH derivatives the direction of nucleobase canting (R for both compounds) is driven by the HT conformer chirality (Δ for both compounds) and not by the chirality of the carrier ligand (*R*,*R* in **1** and *S*,*S* in **2**). Moreover, the degree of canting is much smaller than that observed in analogous compounds with diamine ligands that lack alkyl substituents on the nitrogen atoms (compounds **3** and **4**). Owing to the preference for "six-in" conformations (the six-membered ring of each guanine leans towards the *cis*-G), steric interactions between each guanine H8 and the *cis*-N–Me group are crucial in determining the degree of canting observed. Therefore, in **1** and **2**, which have fully substituted amine nitrogen atoms, the *Φ* angle falls in the range 73–81°, while in analogous compounds that contain primary amine ligands the *Φ* angle is in the range 48–53°.

The theoretical investigation has shown that for a given canting angle the steric interaction between the O6 of each guanine and the *cis* N–Me group is greater for a "quasi axial" than for a "quasi equatorial" methyl group. In contrast, the steric interaction between each guanine H8 and the *cis*-N–Me group is greater for a "quasi equatorial" than for a "quasi axial" methyl group. As a consequence, rotamers that contain O6 or H8 on the same side of the coordination plane as the "quasi equatorial" or "quasi axial" N–Me group, respectively, will be favored in preference to those that have the opposite relationship (O6 and H8 on the same side of the coordination plane as the "quasi axial" or "quasi equatorial" N–Me group, respectively). The preference for the ΔHT conformation, as observed in all the X-ray structures of *cis*-nucleos(t)ide platinum adducts, appears to be governed by a preference for the 5′-terminus of the ribose to be directed towards the *cis*-amine.

The CD investigation clarifies the chiroptic phenomena that arise in *cis*-[PtA_2G_2] model compounds. The major contribution to the CD spectra of HT rotamers in the near UV-visible region (200–350 nm) comes from excitonic couplings between $\pi\rightarrow\pi^*$ transitions of *cis*-guanines. The higher-energy $\sigma\rightarrow\sigma^*$ transitions of the chiral diamine and of the chiral sugar moiety, as well as the $d\rightarrow d$ transitions of the metal have negligible contributions.

For HT rotamers, the $\pi\rightarrow\pi^*$ coupled transition chirality of *cis*-guanines inverts when the disposition of the bases is changed from the Δ to the Λ conformation. This is also the case for the Cotton effect. For the same HT rotamers, the excitonic interaction between *cis*-guanine $\pi\rightarrow\pi^*$ transitions is at a maximum when the nucleobases are perpendicular to the coordination plane. When the nucleobase canting is increased, the intensity of the CD bands diminishes, and the rotational strength actually reaches zero when the two guanosines are disposed into the plane.

The opposite relationship applies for HH rotamers. In the uncanted form, in which the nucleobases are perpendicular to the coordination plane, there is a mirror symmetry plane between the two guanines, and the CD bands that would stem from guanine–guanine interactions have zero intensity. In contrast, if the nucleobases are canted in the coordination plane, the torsion angle between *cis*-guanine $\pi\rightarrow\pi^*$ coupled transitions changes sign as the canting direction changes from right-handed to left-handed. We were unable to confirm this hypothesis for [Pt(Me_4dach)(5′-GMP)$_2$] complexes, because HH rotamers were not formed. However, in compounds that contain CCC ligands, in which a discrete amount of HH rotamer was formed and the nucleobases were considerably canted, the CD spectrum evaluated for the HH rotamer was always much weaker than that observed for the HT forms.

We hope that the present work will be of assistance in the quest to understand the CD spectral features obtained for platinum adducts that interact with long-chain DNA.

Experimental Section

Starting materials: 5′-GMP was used as received, while [Pt{(*R*,*R*)-Me_4-dach}SO_4] and [Pt{(*S*,*S*)-Me_4dach}SO_4] were prepared as previously reported.[36]

ΔHT-[Pt{(*R*,*R*)-Me_4dach}(5′-GMP)$_2$]·10D_2O (1·10D_2O) and ΔHT-[Pt{(*S*,*S*)-Me_4dach}(5′-GMP)$_2$]·14D_2O (2·14D_2O): Stock solutions of 5′-GMP and [Pt{(*R*,*R*)-Me_4dach}SO_4] or [Pt{(*S*,*S*)-Me_4dach}SO_4] (20–30 mM in D_2O) were prepared and adjusted to an acidic pH with diluted D_2SO_4. The selected pH was about 3.0, though a correction for deuterium was not applied. Aliquots of these stock solutions were transferred into an NMR tube to give a final 5′-GMP-to-platinum ratio that was slightly higher than two. The concentration of the platinum complexes in the NMR tubes was in the range of 6–8 mM. The formation of complexes **1** and **2** was monitored by ^{1}H NMR spectroscopy. Crystals of **1**·10D_2O and

2·14 D_2O were separated from the corresponding mother liquor after 3–6 h, as well as after 2–3 weeks from the time the reactants were initially mixed.

A few crystals of each sample were dissolved in D_2O and the ^1H NMR spectrum was obtained. A single set of resonance signals was observed for each compound; this indicates that only one HT rotamer was present. ^1H NMR of **1**: $\delta = 8.29$ (s, 1H; H8), 5.83 (d, $^3J(H,H) = 3$ Hz, 1H; H1′), 4.30 (m, 2H; H2′/H3′), 3.99 (m, 3H; H4′/H5′), 3.28 (m, 1H; CHN), 2.86 (s, 3H; NCH_3), 2.81 (s, 3H; NCH_3), 2.21 and 1.52 (m, 2H; CH_2), 1.75 and 1.24 ppm (m, 2H; CH_2); ^1H NMR of **2**: $\delta = 8.36$ (s, 1H; H8), 5.85 (d, $^3J(H,H) = 6$ Hz, 1H; H1′), 4.44 (m, 1H; H2′), 4.33 (m, 1H; H3′), 4.20 (m, 1H; H4′), 4.08 (m, 2H; H5′), 3.27 (m, 1H; CHN), 2.94 (s, 3H; NCH_3), 2.69 (s, 3H; NCH_3), 2.17 and 1.54 (m, 2H; CH_2), 1.75 and 1.20 ppm (m, 2H; CH_2). The Δ conformation of the HT rotamers was deduced from the CD spectra and confirmed by X-ray crystallography.

Spectroscopy: ^1H NMR spectra were obtained on a Bruker Avance dpx300 instrument. To increase the signal-to-noise ratio, the minimum number of scans per spectrum was 1640. CD and UV/Vis spectra were obtained in the 200–350 nm range on a Jasco J-810 spectropolarimeter. To increase the signal-to-noise ratio, each spectrum was the average of at least 4–16 different scans. After **1** and **2** were crystallized, each mother liquor was enriched with the ΛHT rotamer and it was possible to determine the exact concentrations of the ΛHT and ΔHT rotamers in the mother liquor by NMR spectroscopy. It was then possible to subtract the ΔHT rotamer contribution from the CD spectrum of each mother solution, and, therefore, to evaluate the CD spectrum of the pure ΛHT rotamer (the rotamer ratio was calculated from the NMR data, while the total concentration of platinum species in the CD solution was calculated from the intensity of the corresponding UV/Vis spectrum).

X-ray diffraction

Complex 1·10 D_2O: A freshly prepared well-formed and colorless single crystal ($0.03 \times 0.15 \times 0.15$ mm) was selected under a polarizing microscope and was mounted on a glass capillary. The crystal was covered by a thin layer of cyano-acrylate Super Attack glue and was then used for the data collection procedure; this was performed on a Siemens P4 automatic four-circle diffractometer operating at 293 ± 2 K with graphite monochromated $Mo_{K\alpha}$ radiation ($\lambda = 0.71073$ Å). The data set was corrected for the Lorentz polarization and absorption effect (by means of the ψ-scan technique based on three reflections) with the XSCAN[32] and XEMP[37] computer programs. The selected crystallographic data are listed in Table 1. The accurate cell parameters were determined by the least-squares method; this was applied to the values of 24 randomly selected strong reflections measured in the range $5 \leq 2\theta \leq 18°$. The crystal belongs to the monoclinic system, space group $C2$ (no. 5). Three standard reflections were monitored every 97 reflections; decay was not detected. The R_{int} agreement factor for the intensities (2833) was 0.0192 over 226 equivalencies. The structure solution was performed by direct methods by using SHELXS,[38] and subsequently refined by computing difference Fourier maps and full-matrix least-squares cycles on F^2. All the non-hydrogen atoms were refined anisotropically, whereas the hydrogen atoms (located through the HFIX and AFIX options of SHELXL)[39] were treated as isotropic. The hydrogen atoms of co-crystallized water molecules were not located. The hydrogen atoms of all the water molecules, and those linked to N1 and N2 (guanine moiety), O2′ and O3′ (ribose moiety), as well as O3 (phosphate grouping) were considered as ^2H (deuterium) for the computation of molecular weight and crystallographic parameters. The chirality of the sugar moiety for the refined structure was confirmed from the Flack parameter value [−0.010(6)]. The final R_1 and wR_2 agreement factors for 2607 observed reflections were 0.0207 and 0.0532, respectively [$I > 2\sigma(I)$]. The calculations relevant to the solution and refinement of the structure were performed using the SHELXS[38] and SHELX97[39] packages, whereas the molecular geometry and the molecular graphics analysis was performed using the PARST97,[40] ORTEP32,[41] and XPMA-ZORTEP[42] packages. The tables for the crystallographic data, atomic coordinates, thermal parameters, and geometric parameters were obtained using the CIFTAB program.[43] The computations were performed on Pentium III personal computers.

Complex 2·14 D_2O: A well-formed, colorless prism ($0.25 \times 0.10 \times 0.10$ mm) was selected under the polarizing microscope and was used for the data collection by following the procedure described for **1**. Twenty-six reflections in the range $5 \leq 2\theta \leq 17°$ were used for the cell-constant determination. The crystal belongs to the orthorhombic system, space group $P2_122_1$ (no. 18). The reflections collected (3537) had an R_{int} agreement factor of 0.0088 over 206 equivalencies. The refined Flack parameter was −0.013(6). All the non-hydrogen atoms were refined anisotropically, whereas the hydrogen atoms were treated as isotropic. The hydrogen atoms for the co-crystallized water molecules were not located. Treatment of the ^1H and ^2H atoms was the same as that described above for **1**·10 D_2O. The final R_1 and wR_2 agreement factors were 0.0218 and 0.0572, respectively, over 3331 observed reflections [$I > 2\sigma(I)$].

CCDC 203043 and 203044 contain the supplementary crystallographic data for **1** and **2**, respectively. These data can be obtained free of charge via www.ccdc.cam.ac.uk/conts/retrieving.html (or from the Cambridge Crystallographic Data Centre, 12 Union Road, Cambridge CB2 1EZ, UK; fax: (+44) 1223-336-033; or e-mail: deposit@ccdc.cam.ac.uk).

Computational methods: Single-point density functional calculations at the Becke3LYP/Lanl2dz level,[44] and ab initio calculations at the RHF/Lanl2dz level[44] were performed on the complex molecules **1** and **2** in a canting angle range of 53.2–113.2°. The computations were performed in order to evaluate the total electronic energy of complexes in which the GMP moieties had different orientations with respect to the coordination plane. The package for all the calculations was GAUSSIAN 98,[45] and was implemented on an Origin 3800 Silicon Graphics machine at CINECA (Inter-University Computing Center, Casalecchio di Reno, Bologna, Italy).

Acknowledgements

Professor Luigi G. Marzilli, Department of Chemistry, Louisiana State University, Baton Rouge, is gratefully acknowledged for his critical discussion of the data and for encouraging us in this investigation. Mr. F. Berrettini is gratefully acknowledged for the X-ray data collection at Centro Interdipartimentale di Analisi e Determinazioni Strutturali (CIADS), University of Siena. The Consorzio Interuniversitario per la Ricerca nella Chimica dei Metalli nei Sistemi Biologici (CIRCMSB, Bari) is acknowledged for the grant provided to Gabriella Tamasi. The Ministero dell'Istruzione, dell'Università e della Ricerca (MIUR, PRIN 2001 no. 2001053898), and the Universities of Bari and Siena are acknowledged for funding. The CINECA is acknowledged for Grant 20020306, which allowed the DFT and ab initio calculations to be conducted. Cooperation within COST chemistry projects D20/01/001 and D20/01/003 is gratefully acknowledged.

[1] B. Rosenberg, L. Van Camp, T. Krigas, *Nature* **1965**, *205*, 698–699.
[2] B. Rosenberg, L. Van Camp, E. B. Grimley, A. J. Thomson, *J. Biol. Chem.* **1967**, *242*, 1347–1352.
[3] B. Rosenberg, *Platinum Met. Rev.* **1971**, *15*, 42–51.
[4] R. B. Weiss, M. C. Christian, *Drugs* **1993**, *46*, 360–377.
[5] D. Lebwohl, R. Canetta, *Eur. J. Cancer* **1998**, *34*, 1522–1534.
[6] T. W. Hambley, *Coord. Chem. Rev.* **1997**, *166*, 181–223.
[7] J. Reedijk, *Chem. Commun.* **1996**, 801–806.
[8] E. R. Jamieson, S. J. Lippard, *Chem. Rev.* **1999**, *99*, 2467–2498.
[9] S. O. Ano, Z. Kuklenyik, L. G. Marzilli, in , *Cisplatin: Chemistry and Biochemistry of a Leading Anticancer Drug* (Ed.: B. Lippert) Wiley-VCH, Weinheim, **1999**, pp. 247–291.
[10] L. G. Marzilli, J. S. Saad, Z. Kuklenyik, K. A. Keating, Y. Xu, *J. Am. Chem. Soc.* **2001**, *123*, 2764–2770.
[11] L. G. Marzilli, P. Chalipoyil, *J. Am. Chem. Soc.* **1980**, *102*, 873–875.
[12] M. Gullotti, G. Pacchioni, A. Pasini, R. Ugo, *Inorg. Chem.* **1982**, *21*, 2006–2014.
[13] A. Pasini, L. De Giacomo, *Inorg. Chim. Acta* **1996**, *248*, 225–230.
[14] L. G. Marzilli, F. P. Intini, D. Kiser, H. C. Wong, S. O. Ano, P. A. Marzilli, G. Natile, *Inorg. Chem.* **1998**, *37*, 6898–6905.
[15] H. C. Wong, R. Coogan, F. P. Intini, G. Natile, L. G. Marzilli, *Inorg. Chem.* **1999**, *38*, 777–787.
[16] R. E. Cramer, P. L. Dahlstrom, *J. Am. Chem. Soc.* **1979**, *101*, 3679–3681.
[17] R. E. Cramer, P. L. Dahlstrom, *Inorg. Chem.* **1985**, *24*, 3420–3424.

[18] H. C. Wong, K. Shinozuka, G. Natile, L. G. Marzilli, *Inorg. Chim. Acta* **2000**, *297*, 36–46.
[19] S. Grabner, J. Plavec, N. Bukovec, D. Di Leo, R. Cini, *J. Chem. Soc. Dalton Trans.* **1998**, 1447–1451, and references therein.
[20] R. Cini, S. Grabner, N. Bukovec, L. Cerasino, G. Natile, *J. Chem. Soc. Dalton Trans.* **2000**, 1601–1607.
[21] B. Lippert, *Prog. Inorg. Chem.* **1989**, *37*, 1–97.
[22] L. G. Marzilli, P. Chalipoyil, C. C. Chiang, T. J. Kistenmacher, *J. Am. Chem. Soc.* **1980**, *102*, 2480–2482.
[23] K. J. Barnham, C. J. Bauer, M. J. Djuran, M. A. Mazid, T. Rau, P. J. Sadler, *Inorg. Chem.* **1995**, *34*, 2826–2832.
[24] D. Cremer, J. A. Pople, *J. Am. Chem. Soc.* **1975**, *97*, 1354–1358.
[25] C. Altona, M. Sundaralingam, *J. Am. Chem. Soc.* **1972**, *94*, 8205–8212.
[26] W. Saenger, *Principles of Nucleic Acid Structure*, Springer, Berlin, **1984**.
[27] R. W. Gellert, R. Bau, *J. Am. Chem. Soc.* **1975**, *97*, 7379–7380.
[28] J. D. Orbell, M. R. Taylor, S. L. Birch, S. E. Lawton, L. M. Vilkins, L. J. Keefe, *Inorg. Chim. Acta* **1988**, *152*, 125–134.
[29] S. O. Ano, F. P. Intini, G. Natile, L. G. Marzilli, *Inorg. Chem.* **1999**, *38*, 2989–2999.
[30] Y. Xu, G. Natile, F. P. Intini, L. G. Marzilli, *J. Am. Chem. Soc.* **1990**, *112*, 8177–8179.
[31] The *anti* conformation of the nucleotides appears to be stabilized by an intraligand hydrogen bond between the ribose oxygen O5′ and the C8–H of the guanine base (see text). Moreover, although **1** and **2** do not contain amine protons, rather short distances are found between the phosphate oxygen O2 and the *cis* N–Me groups (see text). Intraligand hydrogen bonds between O(5′) and C8–H were also found in the related compounds **3** and **4**. In these two compounds, the presence of amine protons allowed the formation of strong *cis* amine–phosphate interactions.
[32] XSCAN User Manual, Siemens Analytical X-ray Instruments, Madison, WI, **1994**.
[33] H. C. Wong, F. P. Intini, G. Natile, L. G. Marzilli, *Inorg. Chem.* **1999**, *38*, 1006–1014.
[34] H. Ito, J. Fujita, K. Saito, *Bull Chem. Soc. Jpn.* **1967**, *40*, 2584–2591.
[35] L. B. Clark, B. Leigh *J. Am. Chem. Soc.* **1994**, *116*, 5256–5270, and reference therein.
[36] M. Benedetti, J. S. Saad, L. G. Marzilli, G. Natile, *Dalton Trans.* **2003**, 872–879.
[37] XEMP Empirical Absorption Correction Program, Siemens Analytical X-ray Instruments, Madison, WI, **1994**.
[38] G. M. Sheldrick, SHELXS 97, Program for the Solution of Crystal Structures, University of Göttingen, Germany, **1997**.
[39] G. M. Sheldrick, SHELXL 97, Program for the Refinement of Crystal Structures, University of Göttingen, Germany, **1997**.
[40] M. Nardelli, PARST 97, A System of Computer Routines for Calculating Molecular Parameters from Results of Crystal Structure Analyses, University of Parma, **1997**.
[41] C. K. Johnson, M. N. Burnett, ORTEP-3 for Windows, Oak Ridge National Laboratory, **1998**; 32-bit Implementation by L. J. Farrugia, University of Glasgow.
[42] L. Zsolnai, XPMA-ZORTEP 98, University of Heidelberg, **1998**.
[43] G. M. Sheldrick, CIFTAB Program for the Preparation of Publication Material, University of Göttingen, Germany, **1997**.
[44] A. Frish, M. J. Frisch, *Gaussian 98, User*'s *Reference*, 2nd ed., Gaussian, Inc., Carnegie Office Park, Building 6, Pittsburgh, PA 15106.
[45] M. J. Frisch, G. W. Trucks, H. B. Schlegel, G. E. Scuseria, M. A. Robb, J. R. Cheeseman, V. G. Zakrzewski, J. A. Montgomery, Jr., R. E. Stratmann, J. C. Burant, S. Dapprich, J. M. Millam, A. D. Daniels, K. N. Kudin, M. C. Strain, O. Farkas, J. Tomasi, V. Barone, M. Cossi, R. Cammi, B. Mennucci, C. Pomelli, C. Adamo, S. Clifford, J. Ochterski, G. A. Petersson, P. Y. Ayala, Q. Cui, K. Morokuma, D. K. Malick, A. D. Rabuck, K. Raghavachari, J. B. Foresman, J. Cioslowski, J. V. Ortiz, A. G. Baboul, B. B. Stefanov, G. Liu, A. Liashenko, P. Piskorz, I. Komaromi, R. Gomperts, R. L. Martin, D. J. Fox, T. Keith, M. A. Al-Laham, C. Y. Peng, A. Nanayakkara, M. Challacombe, P. M. W. Gill, B. Johnson, W. Chen, M. W. Wong, J. L. Andres, C. Gonzalez, M. Head-Gordon, E. S. Replogle, J. A. Pople, Gaussian 98, Revision A.7, Gaussian, Inc., Pittsburgh PA, **1998**.

Received: May 19, 2003 [F5152]